Full Paper Wiley Online Library ELECTROANALYSIS

DOI: 10.1002/elan.201500632

Evaluation of Sialic Acid Expression on cancer Cells via an Electrochemical Assay Based on Biocompatible Au@BSA Architecture and Lectin-modified Nanoprobes

Ping Geng,[a] Chongchong Feng,[a] Linling Zhu,[a] Junying Zhang,[a] Fengyang Wang,[a] Kai Liu,[a] Zhiai Xu,*[a] and Wen Zhang*[a]

Abstract: The changes of sialic acid (SA) expression on cell surface are closely associated with various malignant diseases. The analysis of SA expression is therefore becoming an important parameter in clinical diagnosis. In this paper, we reported a sensitive electrochemical cytosensor for the analysis of SA expression on cell surface using three-dimensional architecture of Au@BSA and nanoprobes of carbon nanospheres modified with Au nanoparticles (CNS/AuNPs). Au@BSA microspheres provided an effective matrix for binding of Concanavalin A (Con A) which acted as the recognizer and capturer for cells via the specific affinity to mannose and the core trimannoside of N-glycan on the cell surface. On the basis of the specific recognition of *Sambucus nigra* agglutinin (SNA) to cell surface sialic acid groups, the SNA and HRP modified CNS/AuNPs nanoprobes were introduced onto the electrode surface, and amplified signals were produced by an enzymatic catalytic reaction of HRP toward the oxidation of hydroquinone (HQ) by H_2O_2. This cytosensor was successfully applied to the analysis of SA expression on cell surface disturbed by sialidase and to detect MCF-7 cells and BGC-823 cells with a low detection limit of 40 cells mL^{-1} and 120 cells mL^{-1}. Therefore, the proposed strategy offers a new way for insight into the SA function in biological processes and helps improve cancer diagnosis and treatment.

Keywords: Sialic acid · Cancer cells · Au@BSA · Carbon nanospheres · Cytosensor

1 Introduction

Glycosylation is one of the most crucial post-translational modifications in eukaryotic organisms. It is a dynamic and stage-specific process during many normal and pathological processes including developments and differentiations [1–3]. A large number of glycans covered on cell surfaces play significant roles in many cellular processes, including cell-cell communication, cell growth and development, immune recognition/response, and pathological processes [4–7]. Alterations of glycan expression have been shown to be associated with many diseases such as diabetes, immune deficiencies and especially cancers [8,9]. The investigations indicate that the expression levels of glycans can be used as therapeutic targets or clinical biomarkers for diagnosis of various cancers [10]. Among the diverse structures of glycans, sialic acids (SA) with a nine-carbon backbone are commonly found at the terminal position of the sugar chains. The changes in SA expression level are closely associated with various diseases states such as cancer, cardiovascular and neurological diseases [11]. Therefore, analysis of the cell surface SA expression has become an important subject for understanding their roles in disease development and providing diagnostic tools to guide treatment.

Up to now, a variety of methods have been developed for glycan analysis such as mass spectrometry, high-performance liquid chromatography, nuclear magnetic resonance and capillary electrophoresis [12–15]. Although those approaches can reveal molecular details, they require expensive equipments, much time for sample preparation and are not feasible for profiling surface glycans of living cells due to their destructivity [16]. Recently, lectin-based platforms have been greatly developed for simple and rapid analysis of cell surface glycans [17–19]. These assays mainly rely on the highly specific binding affinities between lectins and corresponding glycans [20]. Among the various lectin-based assays, electrochemical cytosensor has been one of the excellent candidates for the analysis of biological components on living cells because of its simple instrumentation, fast response time and potential ability for real-time and on-site detection [21,22].

In order to fabricate a sensitive electrochemical cytosensor, highly effective immobilization of cells or biomolecules on the electrode surface and enzyme-assisted signal amplification are two significant factors needed to be taken into account. Bovine serum albumin (BSA)-mediated synthesis of inorganic nanomaterials has attracted increasing attention due to the advantages of green reaction process and multi-functionality of the products in

[a] P. Geng, C. Feng, L. Zhu, J. Zhang, F. Wang, K. Liu, Z. Xu, W. Zhang
School of Chemistry and Molecular Engineering, East China Normal University, Shanghai 200241, P. R. China
Phone: +86-21-62232801, +86-21-54340053
*e-mail: zaxu@chem.ecnu.edu.cn
wzhang@chem.ecnu.edu.cn

recent years [23,24]. The outside BSA molecules can not only enhance the amount of biomolecules immobilized on the modified electrode, but also maintain the bioactivity of the immobilized biomolecules. Meanwhile, the inside metal nanoparticles can accelerate the electron transfer process because of their good electric conductivity [25,26]. Enzyme-assisted signal amplification is another critical issue to be focused on. With remarkable development of nanotechnology in materials science, the application of nanomaterials has brought a great momentum in biological assays. Multiple functional nanoprobes integrating the specific glycan recognition and enzyme catalysis were also developed for dynamic electrochemical analysis of cell surface glycans by coupling the nanostructure biointerfaces [27].

Herein, we reported a strategy for the analysis of cell surface SA expression based on Au@BSA as lectin immobilization platform and CNS/AuNPs as signal nanoprobes. The "green-synthesized" Au@BSA nanospheres were synthesized to construct an effective platform with 3-D architecture for anchoring larger amounts of target molecules (Concanavalin A, Con A) with high stability and bioactivity. Moreover, the encapsulated Au nanoparticles (AuNPs) contributed to signal enhancement. Due to the specific recognition of cell surface mannosyl groups to Con A, the Con A/3-D architecture interface displayed a predominant capability for cell capture. Carbon nanospheres (CNSs), with good biocompatibility and tunability of size for loading of biomolecules, were produced by a "green" and cost-effective synthesis under hydrothermal conditions [28,29]. Coupled with AuNPs, the CNS/AuNPs composite were fabricated as a tracing tag to label *Sambucus nigra* agglutinin (SNA) and horseradish peroxidase (HRP) for sensitive immunosensing [30,31]. The accurate evaluation of cell surface SA can be achieved through the selective binding of SNA, a lectin specific to cell surface SA. The analysis of cell surface SA expression was performed based on the catalytic reaction of HRP toward the oxidation of hydroquinone (HQ) by H_2O_2, which could introduce further signal amplification. The proposed cytosensor could respond to the changes of cell surface SA expression disturbed by sialidase. The developed cytosensor based on SA recognition exhibited a better performance for the detection of MCF-7 and BGC-823 cells ranging from 1.0×10^2 to 1.0×10^6 cells mL^{-1} and 5.0×10^2 to 1.0×10^6 cells mL^{-1}, and a low detection limit (40 and 120 cells mL^{-1} for MCF-7 and BGC-823 cells). Therefore, this strategy can not only recognize the cells with high specificity but also detect the cells and its surface SA with high sensitivity. This proposed method offers great promise for the understanding of physiological functions of glycans in the cellular processes as well as the study of clinical diagnosis and therapy of human cancers.

2 Experimental Section

2.1 Materials

Concanavalin A (Con A), *Sambucus nigra* agglutinin (SNA), Poly (diallyldimethylammonium chloride) (PDDA: 20 wt.% in water, Mw: 100 000–200 000), bovine serum albumin (BSA), neuraminidase (sialidase), horseradish peroxidase (HRP) were purchased from Sigma-Aldrich (St. Louis, MO, USA). D-(+)-glucose anhydrous, sodium borohydride, chloroauric acid ($HAuCl_4{\cdot}4H_2O$), ascorbic acid (AA), hydroquinone (HQ), hydrogen peroxide (30 % w/v solution) and other chemical reagents were obtained from Sinopharm Group Chemical Reagent Co., Ltd. (Shanghai, China). Any other solutions were prepared by MilliQ water (18 MΩ·cm, Millipore).

2.2 Apparatus

Electrochemical measurements were performed with a CHI 650C workstation (Chenhua Corp., Shanghai, China) with a conventional three-electrode configuration comprised of a modified Au disk electrode, a platinum wire auxiliary electrode, and a saturated calomel reference electrode (SCE). Cyclic voltammetry (CV) was carried out at a scan rate of 100 mV/s. Electrochemical impedance measurement (EIS) was performed using an alternating current voltage of 5.0 mV, within the frequency range of 0.01 Hz-100 kHz. The UV-vis absorption spectra were obtained from Cary 50 UV-vis-spectrophotometer (Agilent Technologies, Palo Alto, CA). The images of transmission electron microscopy (TEM) and scanning electron microscopy (SEM) were collected from JEM-2100 (JEOL Ltd., Tokyo, Japan) and S-4800 (Hitachi Co., Ltd., Tokyo, Japan), respectively. Fourier transform infrared (FT-IR) spectra were recorded on a Nicolet Nexus 670 instrument (Thermo Nicolet Co., USA) in KBr pellet form.

2.3 Preparation of Au@BSA Microspheres

Au@BSA microspheres were prepared as follows: 50 mg of BSA powder was dissolved in 10 mL of water in a 25 mL beaker under magnetic stirring. Then, an aqueous solution of 10 mM $HAuCl_4$ (10 mL) was added to the BSA solution and allowed to react for 5 min under vigorous stirring at room temperature. After that, 50 mg of ascorbic acid powder was added to the above mixture solution promptly and kept reacting for 5 min under stirring. The obtained reaction product was centrifuged and washed for three times by water and ethanol, respectively. Finally, the product was stored at 4 °C for electrode modification [25].

2.4 Synthesis of CNS/AuNPs Composites

The CNSs were prepared according to the previous protocol through a green method under hydrothermal condi-

tions [28]. In brief, glucose (4 g) was dissolved in water (40 mL) to form a clear solution, which was placed in a teflon-sealed autoclave and maintained at 200 °C for 6 h. The resulting black or puce products were cleaned by three cycles of centrifugation/washing/redispersion in water and in alcohol and oven-dried at 80 °C overnight. Then as-prepared CNSs were treated with a mixture of H_2SO_4/HNO_3 (3 : 1, v/v) by stirring for 2 h to obtain carboxylic group-functionalized CNSs, followed by repeated washing with water until pH 7.0. Subsequently, carboxylated CNSs (1 mg mL^{-1}) were functionalized with PDDA aqueous solution (0.5 %) containing NaCl (0.5 M) by stirring for 40 min to give a homogenous brown suspension. The PDDA/CNSs were obtained by centrifugation and washed with water for three times.

AuNPs were prepared by the reduction of $HAuCl_4$ with trisodium citrate. Briefly, a volume of 100 mL of 0.01 % $HAuCl_4$ in pure water was brought to a boil with vigorous stirring. 2.5 mL of 1 % trisodium citrate was added to the above solution which resulted in a change of color from pale yellow to deep purple within 1–2 min. The mixture was kept boiling for 20 min, and then the solution was allowed to cool to room temperature. The as-prepared AuNPs solution (1 mL) was mixed with PDDA/CNSs (200 µL, 5 mg mL^{-1}). The mixture was then allowed to stand overnight, followed by centrifugation (three times) and redispersion into 1.0 mL solution.

2.5 Preparation of SNA-CNS/AuNPs-HRP Nanoprobes

50 µL of HRP (4 mg mL^{-1}) and SNA (1 mg mL^{-1}) were added to a CNS/AuNPs solution (300 µL) adjusted to pH 9.0 with K_2CO_3 (0.1 M). The mixture was incubated at room temperature with gentle mixing for 2 h. The reaction mixture was then centrifuged at 10,000 rpm for 10 min, and the supernatant was removed. After washing with PBS buffer for three times, the soft sediment was rinsed with PBS (300 µL) containing BSA (1 %) at 4 °C for 30 min. Finally, the conjugate was collected by centrifuging and resuspended in 1 mL of pH 7.4 PBS. The obtained nanoprobes solution was stored in a refrigerator at 4 °C for use.

2.6 Assembly Process of the Electrochemical Cytosensor

The detailed procedure for preparation of the Au@BSA-based electrochemical cytosensor is graphically demonstrated in Scheme 1. Prior to chemical modification, the 2.0 mm Au disk electrode was polished to a mirror-like surface with 0.05 µm alumina powder on microcloth pads and washed ultrasonically in ethanol and water. Then the polished electrodes were immersed into a mixture of a freshly prepared piranha solution (98 % H_2SO_4/30 % H_2O_2, 3 : 1, v/v) for 5 min to remove possible residual contaminant and rinsed with distilled water and ethanol, respectively. After dried under a stream of nitrogen, 3 µL of Au@BSA microspheres (2.5 mg mL^{-1}) was dropped on the surface of Au electrode to construct a biosensing in-

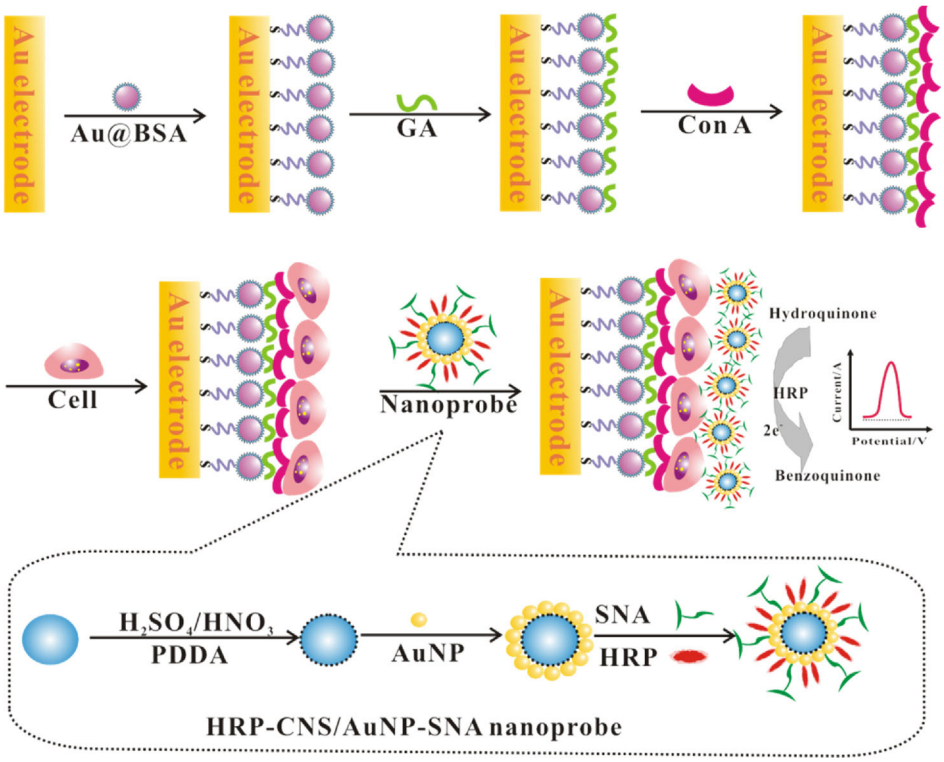

Scheme 1. Schematic representation of the electrochemical cytosensor for the cell surface SA detection.

terface and stored in the refrigerator at 4 °C for 2 h. After thoroughly rinsed with pH 7.4 PBS buffer to remove the unbound microspheres, the Au@BSA-modified Au electrode was coated with 2.5 μL of freshly prepared 12.5 % GA solution at ambient temperature for 1 h. After reaction, the electrode was washed with pH 7.4 PBS buffer. Subsequently, 3 μL of 1 mg mL^{-1} Con A solution was dropped to the film and incubated for 1 h. Then 1 % BSA (w/v) solution was used to block the nonspecific binding sites. Followed by rinsing with buffer, the electrode was soaked in 5 μL of cells suspension at a certain concentration containing 1 mM Ca^{2+} and Mn^{2+}, and was incubated at 37 °C for 1 h to capture the cells via the specific binding between Con A and cell surface mannose and trimannoside groups. After carefully rinsing with PBS to remove the noncaptured cells, the electrode was incubated with 3 μL SNA-CNS/AuNPs-HRP solution for 1 h at 37 °C to form SNA-CNS/AuNPs-HRP/Cells/Con A/Au@BSA/Au electrode. Finally, the electrode was washed thoroughly with PBS to remove non-specifically bound labels.

2.7 Cell Culture and Cell Treatment

The cell lines (BGC-823 and MCF-7) were obtained from Cell Bank of Chinese Academy of Sciences (Shanghai, China). The cells were cultured in a flask in RPMI 1640 medium (GIBCO) supplemented with 10 % fetal calf serum, penicillin (100 μg mL^{-1}), and streptomycin (100 μg mL^{-1}) at 37° in a humidified atmosphere containing 5 % CO_2. L929 mouse fibroblasts were grown in DMEM supplemented with 10 % (v/v) fetal bovine serum (FBS) and 1 wt% penicillin/streptomycin, and incubated in 5 % (v/v) CO_2 under humidified conditions at 37°. The cells in the exponential growth phase were collected and separated from the medium by centrifugation at 1500 rpm for 5 min and then thrice washed with sterile 10 mM pH 7.4 Tris-HCl buffer. The sediment was resuspended in pH 7.4 Tris-HCl buffer (10 mM, containing 1.0 mM Mn^{2+}, 1.0 mM Ca^{2+}, 1.0 mM Na^{+}) to obtain a homogeneous cell suspension. In the drug treatment assay, sialidase-treated cancer cells were obtained by incubating the cells in a culture medium containing 10 μg mL^{-1} sialidase for 24 h.

2.8 Cell Surface SA Measurements

All amperometric measurements were carried out in a conventional three-electrode system composed of a platinum wire as the auxiliary, a saturated calomel electrode as the reference, and a modified Au electrode as the working electrode. The prepared HRP-CNS/AuNPs-SNA/Cells/Con A/Au@BSA/Au electrode was immersed in 5 mL PBS (pH 7.0, 100 mM) solution with 2 mM hydroquinone (HQ) and 1.5 mM H_2O_2. The differential pulse voltammetry (DPV) measurements were performed from – 0.3 to 0.2 V with a pulse amplitude of 50 mV.

3 Results and Discussion

3.1 Characterization of Au@BSA Microspheres

Au@BSA microspheres play a significant role in the preparation of the effective electrochemical cytosensor and the final detection performance. The morphology of Au@BSA was characterized by SEM and TEM. As shown in Figure 1A and 1B, the Au@BSA microspheres

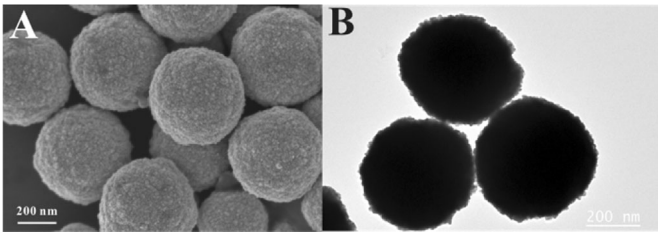

Fig. 1. SEM (A) and TEM (B) images of the prepared Au@BSA microspheres.

displayed spherical morphologies with an average size of 500 nm in diameter and a good monodispersity, which is conducive to develop a homogeneous film on the electrode surface. And the individual gold microsphere is actually composed of aggregated gold nanoparticles, which could greatly promote the electron transfer and improve the detection sensitivity of the fabricated cytosensor. The thin layer (BSA) wrapped outside the microsphere acted as a multifunctional platform to conjugate targeting molecules and block nonspecific binding sites, meanwhile kept the bioactivity of the immobilized biomolecules.

3.2 Characterization of SNA-CNS/AuNPs-HRP Nanoprobes

The CNSs were prepared for the purpose of immobilization of SNA and HRP because of their good monodispersity, large surface area, and versatility for surface functionalization. The SEM images of CNSs displayed good dispersity with average size of approximately 250 nm (Figure 2A). Subsequently, negatively charged AuNPs with 13 nm diameters were electrostatically attached onto the surface of the carboxylated CNSs by using positively charged PDDA as a bridge (Figure 2B). The CNS/AuNPs nanocomposites provided a large capacity for biomacromolecules immobilization and a facile pathway for electron transfer. The SNA-CNS/AuNPs-HRP nanoprobes were further characterized with UV-vis absorption spectroscopy. As seen from Figure 2C, no absorption peak was observed from the CNS/AuNPs nanocomposites (curve a). The characteristic peaks of HRP and SNA appeared at 280 nm and 400 nm (curve b and c). After CNS/AuNPs nanocomposites were modified with SNA and HRP, a distinct absorption peak from SNA and HRP can be observed on the spectra of SNA-CNS/AuNPs-HRP

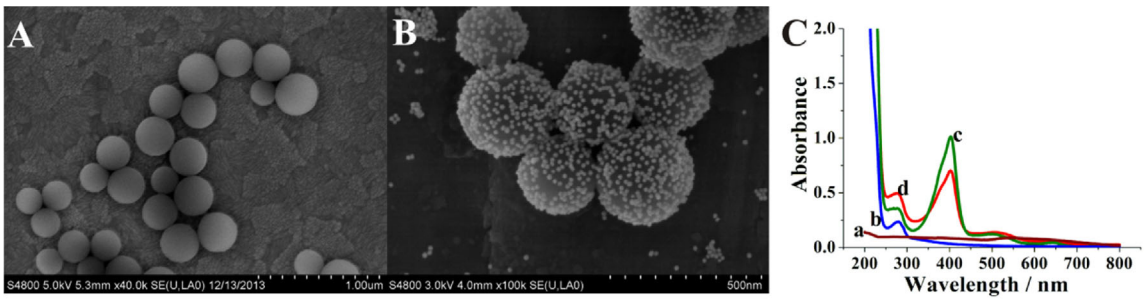

Fig. 2. SEM images of the CNSs (A) and CNSs/AuNPs nanocomposites (B); (C) UV-vis absorption spectra: CNSs/AuNPs (curve a), SNA (curve b), HRP (curve c), SNA-CNS/AuNPs-HRP nanoprobes (curve d).

nanoprobes, which could demonstrate the successful immobilization of HRP and SNA.

3.3 Electrochemical Characterizations of the Cytosensor

The fabrication process of the cytosensor was characterized by electrochemical impedance spectroscopy (EIS) and cyclic voltammetry (CV). Figure 3A illustrates the Nyquist plots of EIS for each stepwise assembly of the cytosensor, which was analyzed in the frequency range 0.1–1.0×10^5 Hz in a phosphate buffer solution (0.01 M, pH 7.4) containing $[Fe(CN)_6]^{3-}/[Fe(CN)_6]^{4-}$ (1:1, 5 mM) as probe. For a bare Au electrode, it showed a R_{et} value of about 150 Ω (curve a). Then Au@BSA microspheres were stably immobilized onto Au electrode surface to construct a 3D sensing layer through the strong effect of Au-S bonds [24]. After the successful assembly of Au@BSA, the R_{et} value decreased to 78 Ω (curve b), which indicated that the presence of Au@BSA could favor the electron transfer. To realize the covalent binding of Con A, GA was utilized as a cross-linking agent. Rapid and quantitative reaction with GA resulted in an increase R_{et} value of 380 Ω (curve c). Subsequently, Con A was conjugated onto the modified film through the "bridge effect" of GA and the R_{et} increased obviously (curve d) because of the poor conductivity of Con A which blocked the electron exchange between the redox probe and the electrode [25]. The further binding of the cells retarded the interfacial electron transfer (curve e), suggesting the specific recognition between Con A and cell surface mannose. Finally, the cytosensor incubated with the SNA-CNSs/Au-HRP nanoprobes for the specific recognition between SNA and cell surface SA. Although the CNSs/Au nanoparticles had excellent conductivity, the nanoprobes of CNSs/Au loading HRP and SNA further blocks the electron transfer on the electrode interface, and an increase in the R_{et} was also observed (curve f). Cyclic voltammetry (CV) was also used to investigate the changes in the electrode behavior after each assembly step and the result was consistent with that from EIS (Figure 3B). Therefore, we believe that Au@BSA on the Au electrode and the CNS/AuNPs not only offered a biocompatible surface for biomolecules loading but also provided a sensitive electric interface for further sensing.

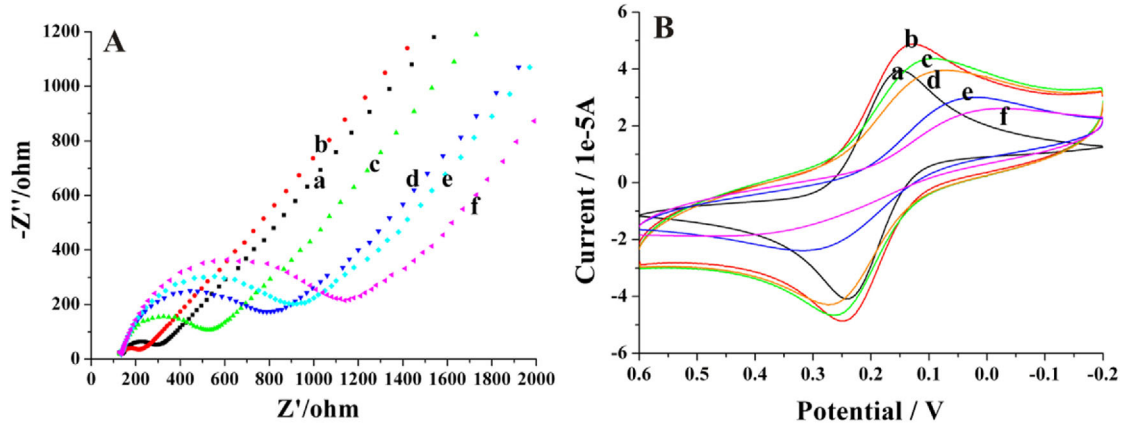

Fig. 3. (A) Nyquist plots of the electrochemical impedance spectroscopy (EIS) at its formal potential with amplitude of 5 mV and frequency range of $0.1–1.0\times10^5$ Hz and (B) Cyclic voltammograms for the fabrication steps: (a) bare Au electrode, (b) Au@BSA/Au electrode, (c) GA/Au@BSA/Au electrode, (d) Con A/GA/Au@BSA/Au electrode, (e) Cells/Con A/GA/Au@BSA/Au electrode, (f) HRP-CNS/AuNPs-SNA/Cells/Con A/GA/Au@BSA/Au electrode. EIS and CV were measured in pH 7.4 PBS containing 5 mM $Fe(CN)_6^{3-/4-}$.

3.4 Optimization of the Experimental Conditions

The incubation time is an important parameter for the target cells capture and the specific recognition of lectins and cells. Figure 4A shows the effects of different incubation time on the DPV response of the immunoassay. The current response increased with increasing incubation time and then levelled off after 60 min, which showed a saturated binding between the cells and lectins. To ensure the completeness of the recognition, 60 min was selected as the optimal incubation time for all the incubation steps of the assay.

The pH also greatly influenced the performance of the electrochemical enzyme-catalyzed analysis. Figure 4B shows the current signal as dependence of the pH of the electrolyte. It was observed that the current responses increased when the pH increased from 6.0 to 7.0 and then decreased when the pH value was further increased to 8.5. Consequently, subsequent experiments employed the PBS of pH 7.0 as the detection solution.

The current response to the concentration of HQ and H_2O_2 was also investigated. As shown in Figure 4C, a significant increase of the current response was observed over a H_2O_2 concentration ranging from 0.5 mM to 1.5 mM, while no obvious difference was obtained for higher concentrations. As for optimizing the HQ concentration, the current response increased with increment of the concentration and then it started to level off after 2 mM (Figure 4D). Therefore, the optimal concentrations of H_2O_2 and HQ for enzyme-amplified DPV detection were 1.5 mM and 2.0 mM, respectively.

3.5 Evaluating Cell Surface SA Expression

Sialic acid on cell surface has been implicated in aggressive cancer cell behavior, and its expression on living cells can provide essential information on cancer status. Thus, we investigated the response of the proposed cytosensor with normal cells (L929 cells), cancer cells (MCF-7 cells) and sialidase-treated cancer cells (sialidase-treated MCF-7 cells). As shown in Fig. 5, the current responses of L929 cells (curve b) are much smaller than those of the MCF-7 cells (curve c), which demonstrated that SA displayed high expression levels in cancer cells as compared to normal cells. The release of SA on cell surface was taken by sialidase, which is usually utilized as a cleaving agent for all forms of SA components present on the carbohydrates of the cell surfaces. The sialidase-treatment leads to more than 90% drop of the current signal (curve d), indicating the decrease of terminal SA on sialidase-treated MCF-7 cells. As a result, the constructed cytosensor provides a high sensitive method for dynamically evaluating cell surface SA expression.

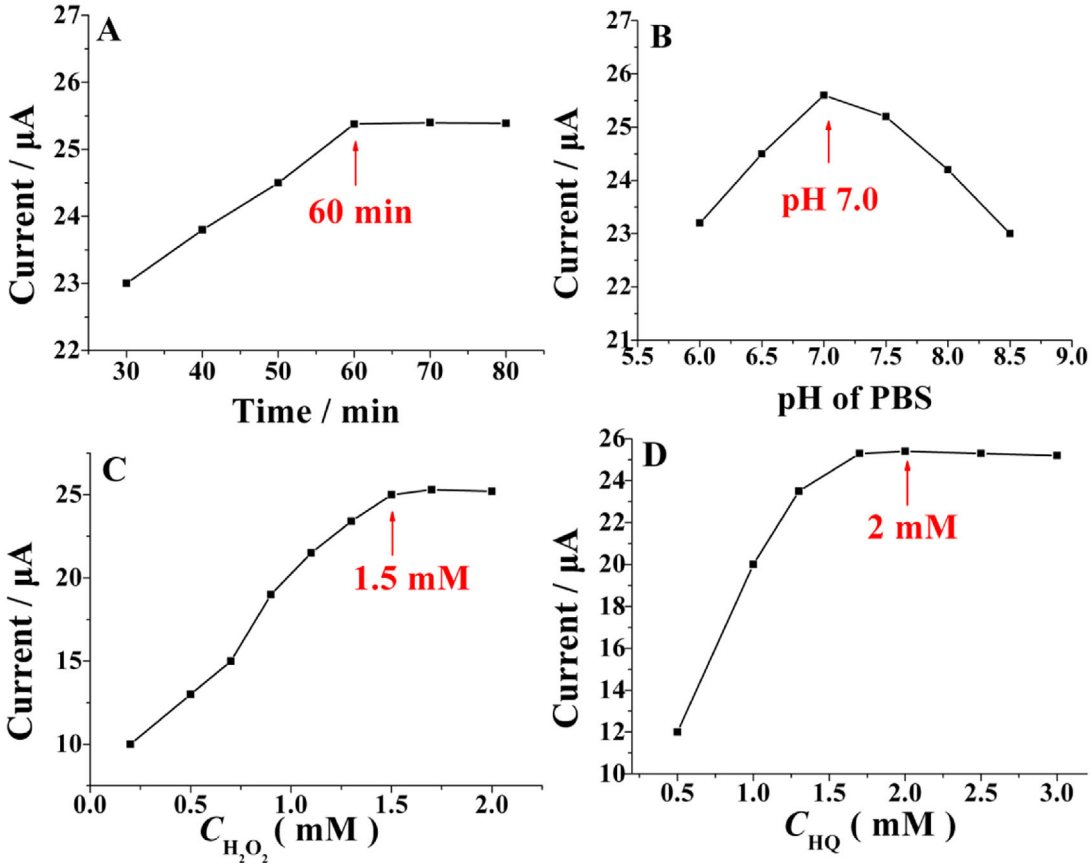

Fig. 4. Influence of (A) incubation time, (B) pH value, (C) the concentration of H_2O_2, and (D) the concentration of HQ on the electrochemical responses of the cytosensor toward MCF-7 cells of 1.0×10^5 cell mL^{-1}.

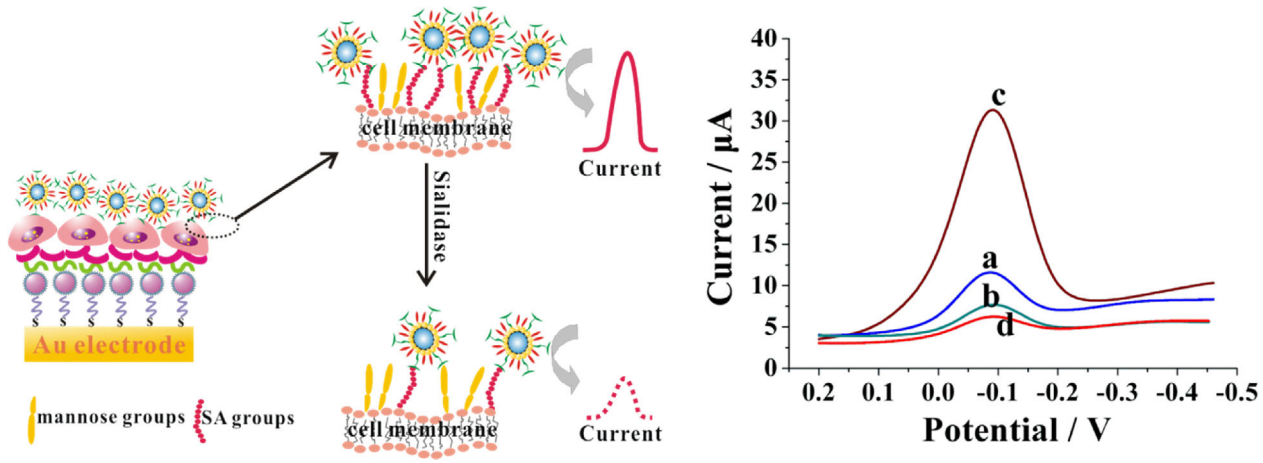

Fig. 5. DPV responses of different types of cells at concentration of 1.0×10^5 cells: (a) blank control of pH 7.4 PBS, (b) L929 cells, (c) MCF-7 cells, (d) sialidase-treated MCF-7 cells.

3.6 Quantitative Detection of Cancer Cells with the Cytosensor

High sensitive detection of cancer cells is extremely important for early cancer diagnosis and thus greatly increases the chance for effective treatment. In view of the above challenges, we used the proposed cytosensor for the quantification of cancer cells (MCF-7 and BGC cells). Figure 6A shows the DPV curves of the cytosensor in the presence of MCF-7 cells (breast cancer cells) with different concentrations. When the concentration of cancer cells increased, the current response enhanced according-

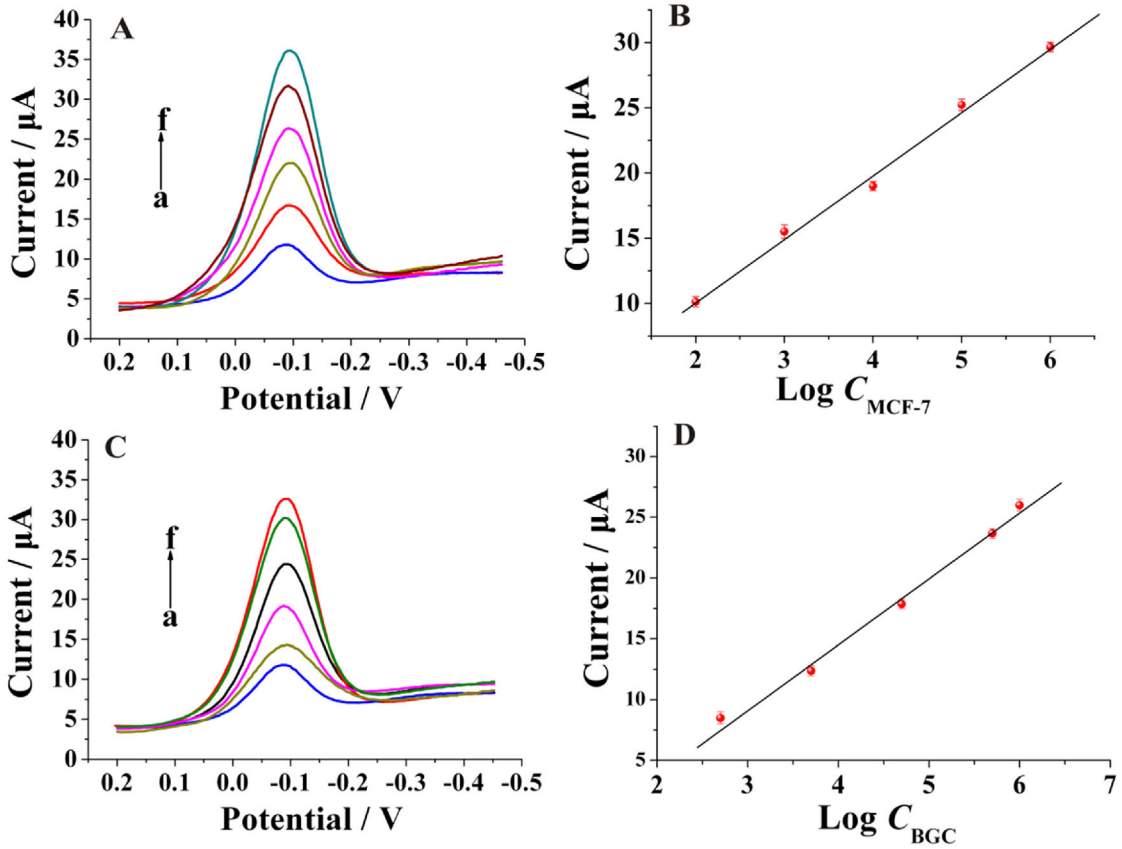

Fig. 6. (A) DPV responses at various concentrations of MCF-7 cells: (a) 0, (b) 1.0×10^2 cells, (c) 1.0×10^3 cells, (d) 1.0×10^4 cells, (e) 1.0×10^5 cells, (f) 1.0×10^6 cells. (B) The calibration curve for SA analysis on MCF-7 cells. (C) DPV responses at various concentrations of BGC-823 cells: (a) 0, (b) 5.0×10^2 cells, (c) 5.0×10^3 cells, (d) 5.0×10^4 cells, (e) 5.0×10^5 cells, (f) 1.0×10^6 cells. (D) The calibration curve for SA analysis on BGC-823 cells.

Table 1. Assay results of cancer cells with the proposed cytosensor.

Cell	Linear regression equation	Linear range (cells mL^{-1})	R
MCF-7	$i_p(\mu A) = 4.874 \log C_{MCF\text{-}7} + 0.414$	1.0×10^2–1.0×10^6	0.994
BGC-823	$i_p(\mu A) = 5.332 \log C_{BGC\text{-}823} - 6.634$	5.0×10^2–1.0×10^6	0.991

ly. The calibration plot showed a good linear relationship between the current response and the logarithmic value of the MCF-7 cells concentration in the range from 1.0×10^2 cell mL^{-1} to 1.0×10^6 cell mL^{-1} (Figure 6B). The linear regression equation was i_p (μA) $= 4.874 \log C_{MCF\text{-}7} + 0.414$ with a correlation of 0.994. The detection limit for the cell concentration was estimated to be 40 cell mL^{-1}. Meanwhile, the SA expression on BGC-823 cells (human gastric cancer cells) was also evaluated (Figure 6C and 6D) and the obtained results are summarized in Table 1. The detection limit for the BGC-823 cells was estimated to be 120 cell mL^{-1}.

The reproducibility of the proposed cytosensor was evaluated from the DPV response of three independently made cytosensors with same cell concentration. The current response gave a relative standard deviation (R.S.D) of 4.2% for the examinations at the MCF-7 cell concentration of 1.0×10^5 cells mL^{-1}. These results indicated that the proposed cytosensor exhibited good performance in analyzing cancer cells with a satisfactory detection range, low detection limit and good reproducibility. It is obvious that the sensitivity of the cytosensor with specific carbohydrate identification and enzymatic catalysis is higher than or comparable with those of lectin-based electrochemical biosensors for cancer cell determination [1,17–19,21]. Therefore, the proposed cytosensor displays good performance in cancer cell detection and is promising in the studies of histopathological lesion process.

4 Conclusions

In this paper, we have successfully exploited a sensitive electrochemical cytosensor for cell surface SA analysis by employment of a dual signal amplification strategy. The Au@BSA can not only enhance the electron transfer ability but also provide a multivalent recognition interface for the conjugation of Con A. The cell capture was realized by the highly specific binding affinity of Con A to cell surface mannose. The CNS/AuNPs nanocomposites were adopted as carriers to link SNA and HRP for subsequent electrochemical assay. The analysis of cell surface SA expression relied on the specific binding affinity of SNA to cell surface SA. This strategy integrated the merits of Au@BSA platform, enzyme-assisted signal amplification, and electrochemical measurement, and demonstrated that the presented method had excellent performance with high sensitivity and specificity for the analysis of cell surface SA expression. Therefore, the proposed method offers a great promise for the understanding of SA function in biological processes and related diseases, which will improve successful clinic diagnosis and treatment.

Acknowledgements

This work was financially supported by the National Natural Science Foundation of China (No. 21375040, 21305047, 21205051).

References

[1] A. Matsumoto, N. Sato, K. Kataoka, Y. Miyahara, *J. Am. Chem. Soc.* **2009**, *131*, 12022.
[2] Z. Dai, A. Kawde, Y. Xiang, J. T. La Belle, J. Gerlach, V. P. Bhavanandan, L. Joshi, J. Wang, *J. Am. Chem. Soc.* **2006**, *128*, 10018.
[3] P. M. Rudd, T. Elliott, P. Cresswell, I. A. Wilson, R. A. Dwek, *Science* **2001**, *291*, 2370.
[4] K. Ohtsubo, J. D. Marth, *Cell*, **2006**, *126*, 855.
[5] J. D. Marth, P. K. Grewal, *Nat. Rev. Immunol.* **2008**, *8*, 874.
[6] Y. Kinjo, D. Wu, G. Kim, G. W. Xing, M. A. Poles, D. D. Ho, M. Tsuji, K. Kawahara, C. H. Wong, M. Kronenberg, *Nature* **2005**, *434*, 520.
[7] E. Han, L. Ding, R. Qian, L. Bao, H. X. Ju, *Anal. Chem.* **2012**, *84*, 1452.
[8] D. H. Dube, C. R. Bertozzi, *Nat. Rev. Drug Discov.* **2005**, *4*, 477.
[9] Y. Zhang, E. P. Go, H. Desaire, *Anal. Chem.* **2008**, *80*, 3144.
[10] Y. Matsuno, T. Saito, M. Gotoh, H. Narimatsu, A. Kameyama, *Anal. Chem.* **2009**, *81*, 3816.
[11] A. Liu, S. Peng, J. C. Soo, M. Kuang, P. Chen, H. Duan, *Anal. Chem.* **2011**, *83*, 1124.
[12] L. Royle, M. P. Campbell, C. M. Radcliffe, D. M. White, D. J. Harvey, J. L. Abrahams, Y. G. Kim, G. W. Henry, N. A. Shadick, M. E. Weinblatt, D. M. Lee, P. M. Rudd, R. A. Dwek, *Anal. Biochem.* **2008**, *376*, 1.
[13] K. Kaneshiro, M. Watanabe, K. Terasawa, H. Uchimura, Y. Fukuyama, S. Iwamoto, T. A. Sato, K. Shimizu, G. Tsujimoto, K. Tanaka, *Anal. Chem.* **2012**, *84*, 7146.
[14] W. A. Bubb, *Concepts Magn. Reson. Part A* **2003**, *19A*, 1.
[15] Y. Mechref, M. V. Novotny, *Mass Spectrom. Rev.* **2009**, *28*, 207.
[16] K. T. Pilobello, L. K. Mahal, *Curr. Opin. Chem. Biol.* **2007**, *11*, 300.
[17] S. Y. Chen, T. Zheng, M. R. Shortreed, C. Alexander, L. M. Smith, *Anal. Chem.* **2007**, *79*, 5698.
[18] J. J. Zhang, F. F. Cheng, T. T. Zheng, J. J. Zhu, *Anal. Chem.* **2010**, *82*, 3547.
[19] Z. H. Chen, Y. Liu, Y. Z. Wang, X. Zhao, J. H. Li, *Anal. Chem.* **2013**, *85*, 4431.
[20] H. Lis, N. Sharon, *Chem. Rev.* **1998**, *98*, 637.
[21] X. Zhang, Y. Teng, Y. Fu, L. Xu, S. Zhang, B. He, C. Wang, W. Zhang, *Anal. Chem.* **2010**, *82*, 9455.
[22] Y. L. Zhang, Y. Huang, J. H. Jiang, G. L. Shen, R. Q. Yu, *J. Am. Chem. Soc.* **2007**, *129*, 15448.
[23] C. Y. Hu, D. P. Yang, Z. H. Wang, P. Huang, X. S. Wang, D. Chen, D. X. Cui, M. Yang, N. Q. Jia, *Biosens. Bioelectron.* **2013**, *41*, 656.
[24] A. V. Singh, B. M. Bandgar, M. Kasture, B. Prasad, *J. Mater. Chem.* **2005**, *15*, 5115.

[25] C. Y. Hu, D. P. Yang, Z. Y. Wang, L. L. Yu, J. L. Zhang, N. Q. Jia, *Anal. Chem.* **2013**, *85*, 5200.
[26] C. Y. Hu, D. P. Yang, K. Xu, H. M. Cao, B. N. Wu, D. X. Cui, N. Q. Jia, *Anal. Chem.* **2012**, *84*, 10324.
[27] R. S. Haltiwanger, J. B. Lowe, *Annu. Rev. Biochem.* **2004**, *73*, 491.
[28] X. Sun, Y. Li, *Angew. Chem. Int. Ed.* **2004**, *43*, 597.
[29] L. R. Kong, X. F. Lu, X. J. Bian, W. J. Zhang, C. Wang, *Langmuir* **2010**, *26*, 5985.
[30] Q. Xu, F. Yan, J. Lei, C. Leng, H. Ju, *Chem. Eur. J.* **2012**, *18*, 4994.
[31] W. P. Li, L. Li, S. G. Ge, X. R. Song, L. Ge, M. Yan, J. H. Yu, *Chem. Commun.* **2013**, *49*, 7687.

Received: September 24, 2015
Accepted: October 30, 2015
Published online: ■■ ▮▮, 0000

FULL PAPERS

P. Geng, C. Feng, L. Zhu, J. Zhang, F. Wang, K. Liu, Z. Xu, W. Zhang**

■■–■■

Evaluation of Sialic Acid Expression on cancer Cells via an Electrochemical Assay Based on Biocompatible Au@BSA Architecture and Lectin-modified Nanoprobes